DOI: 10.1002/ejoc.200701115

# Functionalized 2,5-Dipyridinylpyrroles by Electrochemical Reduction of 3,6-Dipyridinylpyridazine Precursors

Hicham Bakkali,[a,b] Cécile Marie,[a,b] Akarim Ly,[c] Christine Thobie-Gautier,[a,b] Jérôme Graton,[a,b] Muriel Pipelier,[a,b] Stéphane Sengmany,[d] Eric Léonel,[d] Jean-Yves Nédélec,[d] Michel Evain,[e] and Didier Dubreuil*[a,b]

**Keywords:** Nitrogen heterocycles / Ring contraction / Electrochemistry / Reduction

The ring contraction of pyridinylpyridazine derivatives into the corresponding pyrroles by electrochemical reduction was studied, and the influence of the substituents of the pyridazine precursors on the process is discussed. Cyclic voltammetry studies underlines the electron-withdrawing or -donating effect of the substituent on the pyridazine ring, which determines the reaction pathway of their preparative electrolysis. The ring-contraction process, with extrusion of nitrogen, proceeds by two subsequent two-electron, two-proton processes via a 1,2-dihydropyridazine intermediate. The latter can either rearrange into an isolable 1,4-dihydropyridazine or undergo formation of pyrroles by disproportionation or by a second electrochemical reduction involving two-electrons and two protons. X-ray structure, fluorescence spectra, and conformational analysis of pyridinylpyrrole sequences supported this study.


## Introduction

Pyrroles are very important heterocycles used in materials science,[1] especially when incorporated into conjugated chains, because of their conducting and optical properties.[2,3] Pyrroles are also involved as structural moieties in many naturally occurring biologically active compounds[4] such as marine pyrrole-based alkaloids[5] and pyrrole–imidazole alkaloids,[6] and they have gained importance in the field of medicinal chemistry.[7]

Among the many strategies available to form pyrrole derivatives, chemical ring contraction of larger rings is one important tool that has long been described in the literature.[7] This methodology affords pyrrole derivatives with varied substituents, which are otherwise difficult to synthesize. Recently, we showed that electrochemical transformations of 3,6-bis(methoxycarbonyl)pyridazines **1** in an acidic medium proceeds by a four-electron reduction process to give the corresponding 2,5-bis(methoxycarbonyl)pyrroles **5** according to the mechanism shown in Scheme 1.[8,9]

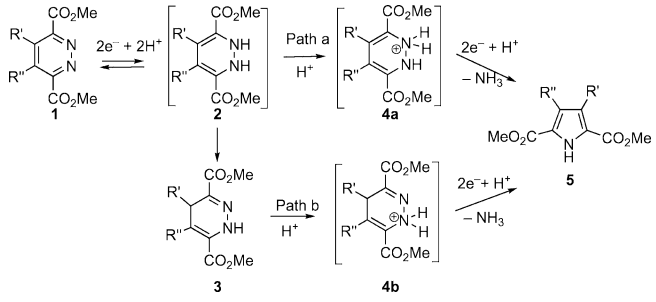


Scheme 1. Mechanism for the electrochemical reduction of bis-(methoxycarbonyl)pyridazines.

The electrochemical reduction of 4,5-substituted 3,6-bis-(methoxycarbonyl)pyridazines **1** affords a mixture of 1,4-dihydropyridazines **3** and pyrroles **5**, according to the nature of the C4 and C5 substituents (R′ and R′′). The product distribution is governed by the chemical behavior of the 1,2-dihydropyridazine intermediate **2** formed by the first two-electron reduction of the pyridazine precursor **1**. Dihydropyridazine **2** can either be oxidized back into the starting material, as clearly shown by cyclic voltammetry,[9] or rearrange into the 1,4-dihydropyridazine **3**. Both dihydropyridazine intermediates **2** and **3** can be further reduced by another two-electron process to give the corresponding pyrrole **5** by two different chemical pathways a and b via the corresponding iminium intermediates **4a** and **4b**, respectively (Scheme 1). Moreover, 1,2-dihydropyridazine **2** can

[a] Université de Nantes, CEISAM, Chimie Et Interdisciplinarité, Synthèse, Analyse, Modélisation, UFR des Sciences et des Techniques,
2 rue de la Houssinière, B. P. 92208, 44322 Nantes Cedex 3, France
[b] CNRS, UMR CNRS 6230
2 rue de la Houssinière, B. P. 92208, 44322 Nantes Cedex 3, France
[c] Département de Génie Chimique, Université de Conakry, Guinea
[d] Electrochimie et Synthèse Organique, Institut de Chimie et des Matériaux Paris-Est UMR 7182 – CNRS, Université Paris 12, 2 rue Henri-Dunant, 94320 Thiais, France
[e] Université de Nantes, Nantes Atlantique Universités, CNRS, Faculté des Sciences et des Techniques, Institut des Matériaux Jean Rouxel, UMR CNRS 6502,
2 rue de la Houssinière, B. P. 92208, 44322 Nantes Cedex 3, France

  

also disproportionate into the starting pyridazine and the expected pyrrole. If the isomerisation of **2** into **3** is fast, the amount of pyrrole can be considerably decreased, as the electroreduction of 1,4-dihydro derivative **3** is not the favored way to form pyrroles.

It comes out that the electrochemical process is very sensitive to the nature of the functionalities on the substrate. Indeed, 3,6-bis(methoxycarbonyl)pyridazine bearing a phenyl group at C4 allowed the formation of the corresponding pyrrole in 70% high yield, whereas the 3,4,5,6-tetrakis(methoxycarbonyl) analogue gives rise to the corresponding 1,4-dihydro derivative **3** as the sole product.

We investigated a complementary study of a C4 substituent effect on the electrochemical reduction of 3,6-dipyridinylpyridazines providing functionalized 3,6-dipyridinylpyrrole analogues. The study was carried out in comparison with the conventional chemical ring-contraction procedure extensively used by Boger (Zn/AcOH in acidic medium).[10,11] The interest of the synthesis of such a substituted dipyridinylpyrrole sequence is highlighted by a variety of applications of biological interest,[12,13] or as potent anionic complex agents with organometals,[14] or as cationic ligands when linked to amidinium or guanidinium salts to allow interaction with DNA or RNA sequences.[15,16]

## Results and Discussion

### Preparation of the Dipyridinylpyridazine Precursors

The preparation of 4-substituted 3,6-dipyridin-2-ylpyridazines and -4-ylpyridazines **9**–**14** and those of 3,6-bis(6-methylpyridin-2-yl- and -4-yl)pyridazines **15**–**17** was carried out following a well-described procedure from 2- and 4-cyanopyridine precursors (Scheme 2).[15,17,18] Diels–Alder reactions from 3,6-dipyridinyltetrazine intermediates **6**, **7**, or **8** in the presence of various dienophiles led to the targeted pyridazines **9**–**17** in good yields after extrusion of molecular nitrogen (Table 1).

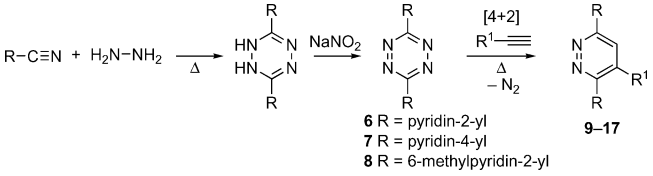


Scheme 2. Pyridazine synthetic pathway.

Table 1. Yield of pyridazines obtained by Diels–Alder reaction.

| Pyridazine | R | $R^1$ | Yield [%] | Ref. |
|---|---|---|---|---|
| **9** | pyridin-2-yl | H | 92 | [19,20] |
| **10** | pyridin-2-yl | $(CH_2)_3CH_3$ | 91 | [20] |
| **11** | pyridin-2-yl | $(CH_2)_2OH$ | 71 | [20] |
| **12** | pyridin-2-yl | $OC_2H_5$ | 40 | |
| **13** | pyridin-2-yl | $(CO_2)C_2H_5$ | 82 | [21] |
| **14** | pyridin-4-yl | H | 93 | |
| **15** | 6-methylpyridin-2-yl | H | 98 | |
| **16** | 6-methylpyridin-2-yl | $(CH_2)_3CH_3$ | 84 | |
| **17** | 6-methylpyridin-2-yl | $(CO_2)C_2H_5$ | 97 | |

### Electrochemical Behavior of the Substituted Pyridazines

In our previous study,[9] we showed that the electrochemical reduction of 3,6-bis(methoxycarbonyl)pyridazine proceeds in three successive bielectronic steps [$E_{1/2}$ = –0.69, –0.86, –1.07 V/SCE (saturated calomel electrode)] with a reversibility of the first step in cyclic voltammetry in acetate buffer/ethanol (1:1) at a scan rate of 0.2 $V s^{-1}$. Moreover, when the potential was scanned down to the level of the second wave ($E_{1/2}$ = –0.86 V/SCE), a new reversible step was observed at a more anodic potential at around +0.1 V/SCE.

Also, in our previous experiments carried out on 3,6-dipyridinylpyridazines **9** and **14**,[9] we found that the first polarographic reduction wave ($E_{1/2}$ = –0.75 V/SCE) corresponds to an irreversible four-electron transfer, whereas the next two waves are not well defined and are masked by adsorption peaks.

We have now complemented this previous study by the electrochemical investigation of the substituted dipyridinylpyridazines **9**–**17** in acetate buffer/ethanol medium to establish the favorable general conditions for their controlled potential electrolysis. In each case, the polarography or cyclic voltammetry experiments[22] displayed three defined irreversible steps.

Figure 1 shows the cyclic voltammograms of pyridazine **9**, used as a reference model, at a glassy carbon electrode in acetate buffer/ethanol at two different scan rates (0.2 $V s^{-1}$ Figure 1A and $2 \times 10^{-3}$ $V s^{-1}$ Figure 1B). Voltammetry performed at a mercury electrode or a solid glassy carbon electrode gave the same profile despite an anodic potential shift (0.04 V) with the mercury electrode. Therefore, the glassy carbon electrode was selected for the voltammetry studies.

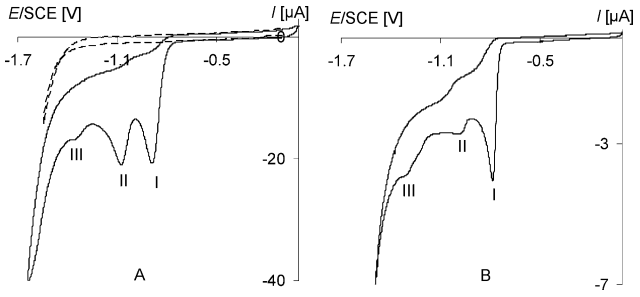


Figure 1. Cyclic voltammograms at a glassy carbon electrode in acetate buffer/ethanol (1:1) (---) and in the presence of **9** (—) ($C$ = $10^{-3}$ mol $L^{-1}$) at a scan rate of 0.2 $V s^{-1}$ (A) and $2 \times 10^{-3}$ $V s^{-1}$ (B).

The cyclic voltammogram of 3,6-dipyridin-2-ylpyridazine **9** recorded at 0.2 $V s^{-1}$ displays two well-defined irreversible cathodic peaks (I and II) along with a poorly defined wave at a more cathodic potential (III). It is important to notice that no reversibility is observed at any reduction step, contrary to the reversibility reported in the case of 3,6-bis(methoxycarbonyl)pyridazines.[9] On the basis of our mechanistic hypothesis, peak I, at $E_{pI}$ = –0.88 V/SCE, corresponds to the first two-electron reduction of pyridazine, which leads to a 1,2-dihydropyridazine intermediate, whereas peak II ($E_{pII}$ = –1.06 V/SCE) represents the second

  

two-electron reduction of the latter into the pyrrole ring. Furthermore, the last wave III can be assigned to the reduction of the pyrrole derivative. That was confirmed by the cyclic voltammogram of the pure pyrrole **18**, which presents a single cathodic peak at –1.35 V/SCE. Consequently, the first two peaks I and II, which illustrate the four-electron and four-proton transfers, are assignable to the complete transformation of the pyridazine ring into pyrrole following the extrusion of a nitrogen atom (Scheme 3, Path a). Would the process follow Path a, however, we should have the two peaks I and II of the same current intensity corresponding to two two-electron processes. This is not observed, and the ratio of $Ip_I/Ip_{II}$ is 2.5, which thus indicates more than two and less than four as the electrons transferred at wave I. At a lower scan rate of 2 mV s$^{-1}$, the peak ratio is even greater, and peak III is also more intense. These observations can be explained by a poor stability in acidic solution of the first-formed 3,6-dipyridin-2-yl-1,2-dihydropyridazine intermediate and its rather rapid disproportionation into the starting pyridazine and the pyrrole (Scheme 3, Path b), which thus accounts for the increase in the current intensities of peaks I and III, respectively.[8,9]

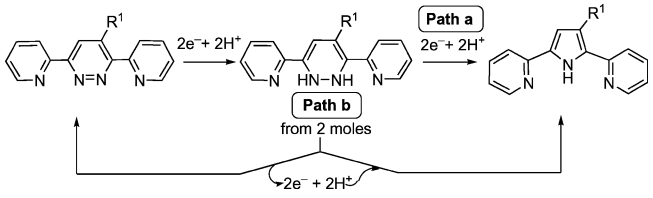


Scheme 3. General transformation pathway of pyridazines into pyrroles.

The effects of the substitution ($R^1$) of the pyridazine moieties on their electrochemical behavior were then evaluated in comparison with pyridinylpyridazine **9** and 6-methylpyridinylpyridazine **15**, used as reference compounds ($R^1$ = H). Table 2 reports the data for the first two cathodic peaks I and II measured for the two series **10**–**13** and **16**–**17** (the ratio $Ip_I/Ip_{II}$ was determined at a scan rate of 0.2 V s$^{-1}$).

We noticed that the reduction potential values are only slightly influenced by the nature of $R^1$. As expected, and in comparison to the cyclic voltammograms of pyridazine **9**, a small negative potential shift was induced by an electron-donating group (**10**–**12**) and vice versa in the presence of an electron-withdrawing group (**13**). Moreover, a large variation in the current intensity of peaks I and II was observed depending on the nature of $R^1$. Cyclic voltammograms of pyridazines **10** and **13** bearing an electron-donating (Bu) and electron-withdrawing substituent ($CO_2Et$), respectively, illustrate the actual trends (Figure 2).

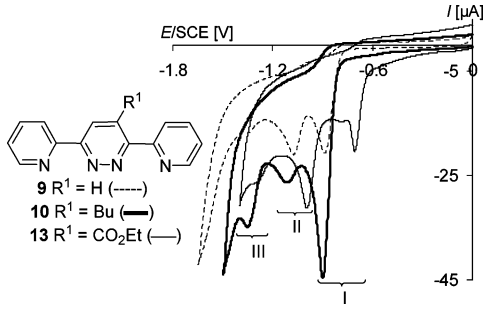


Figure 2. Cyclic voltammograms at a glassy carbon electrode in acetate buffer/ethanol (1:1) of compounds **9** (---), **10** (—), and **13** (—) ($C$ = 10$^{-3}$ mol L$^{-1}$) at a scan rate of 0.2 V s$^{-1}$.

The effect of an electron-donating group ($R^1$ = Bu, **10**; $R^1$ = $C_2H_4OH$, **11**) results in a significant increase in the current of peak I relative to the current of peak II ($Ip_I/Ip_{II}$ = 10). This observation indicates that, after the first reduction step, the 1,2-dihydropyridazine intermediates evolve rapidly in acidic medium to give the expected pyrroles **19** and **20**, respectively, either after another two-electron reduction (Scheme 3, Path a) or by disproportionation (Scheme 3, Path b). However, the decrease in the $Ip_I/Ip_{II}$ ratio to 3 in the presence of an OEt donating group highlighted the sensibility of the equilibrium of the processes and anticipates different behaviors under preparative electrolyses.

In the case of an electron-withdrawing substituent ($R^1$ = $CO_2Et$, **13**), current intensities of peaks I and II are nearly equal ($Ip_I/Ip_{II}$ = 1.3). This result is explained by stabilization of the 1,2-dihydropyridazine intermediate by the substituent. Consequently, the reduction of the latter to the corresponding pyrrole **22** by consuming two more electrons and two more protons (Scheme 3, Path a) is in competition with the formation of the 1,4-dihydropyridazine intermediate.

Differences in the potential observed between the first two reduction peaks ($\Delta Ep$) also led to the same conclusion. Indeed, the values of $\Delta Ep$ are smaller in the case of elec-

Table 2. Cyclic voltammetry data of substituted pyridazines at a glassy carbon electrode, $E_p$ (V/SCE) and $v$ = 0.2 V s$^{-1}$.

| Pyridazine | R | $R^1$ | $Ep_I$ | $Ep_{II}$ | $\Delta Ep$[a] | $Ip_I/Ip_{II}$ |
|---|---|---|---|---|---|---|
| **9** | pyridin-2-yl | H | –0.88 | –1.06 | 0.18 | 2.5 |
| **10** | pyridin-2-yl | $(CH_2)_3CH_3$ | –0.89 | –1.08 | 0.19 | 10 |
| **11** | pyridin-2-yl | $(CH_2)_2OH$ | –0.92 | –1.11 | 0.19 | 10 |
| **12** | pyridin-2-yl | $OC_2H_5$ | –0.99 | –1.18 | 0.19 | 3 |
| **13** | pyridin-2-yl | $CO_2C_2H_5$ | –0.71 | –0.99 | 0.28 | 1.3 |
| **14** | pyridin-4-yl | H | –0.79 | –0.97 | 0.18 | 2 |
| **15** | 6-methylpyridin-2-yl | H | –0.83 | –1.01 | 0.18 | 2.5 |
| **16** | 6-methylpyridin-2-yl | $(CH_2)_3CH_3$ | –0.85 | –1.05 | 0.20 | 15 |
| **17** | 6-methylpyridin-2-yl | $CO_2C_2H_5$ | –0.71 | –1.01 | 0.30 | 1 |

[a] $\Delta Ep = Ep_{II} - Ep_I$.

  

tron-donating substituents ($\Delta Ep \approx 0.19$ V for **10**–**12**) than for electron-withdrawing groups ($\Delta Ep \approx 0.28$ V for **13** and $\Delta Ep \approx 0.30$ V for **16**), which confirms a preferred dismutation occurrence in the presence of electron-donating groups.

Similar results were obtained in the (6-methylpyridinyl)-pyridazine series **15**–**17** ($\Delta Ep \approx 0.18$, 0.20, 0.30; $Ip_I/Ip_{II}$ = 2.5, 15, 1.0, respectively, for **15**, **16**, **17**), which underlines that the methyl substituent on the pyridinyl group does not have a significant influence on the electrochemical behavior of the pyridazines.

These observations highlighted the versatility of the electrochemical process related to the nature of the substituents present at different positions on the pyridazine precursors, and this was considered complementary to what was already established in the literature, which was that electron-donating groups at the 3,6-positions disfavor the ring-contraction process. Consequently, the variation in the yield of 2,5-dipyridinylpyrrole formation by preparative electrolyses of 3,6-dipyridinylpyridazine should be anticipated.

### Preparative Electrolyses of Substituted Pyridazines

In order to optimize the electrochemical formation of pyrrole derivatives, a series of controlled potential electrolyses of pyridazines **9** to **17** was performed at the second reduction peak potential ($Ep_{II}$). The experiments were carried out in a mixture of acetate buffer (pH = 4.6) and ethanol (1:1) at a mercury pool cathode in the two-compartment cell by using a glass frit. The results of electrochemical reductions are summarized in Table 3 along with, for comparison, the yields obtained by the alternative ring-contraction chemical procedure (Scheme 4). Reactions were monitored by cyclic voltammetry measurement within the cathodic compartment and the electrolyses stopped when the starting substrate was consumed. Then, all preparative electrolyses were performed within 4–6 h, compared to the18 h required under chemical Zn/AcOH conditions.

Table 3. Coulometric data and yields of substituted pyrroles by electrochemical or chemical syntheses.

| Pyridazine | $n$ [F mol$^{-1}$] | Time [h] CPE | Pyrrole | Yield [%] CPE[a] | Yield [%] Zn/AcOH |
|---|---|---|---|---|---|
| **9** | 4.1 | 4.6 | **18** | 82 | 22 |
| **10** | 4.5 | 6.0 | **19** | 87 | 18 |
| **11** | 4.5 | 5.3 | **20** | 92 | 15 |
| **12** | 4.5 | 5.2 | **21** | 68 | 30 |
| **13** | 5.6 | 6.2 | **22** | 53 | 37 |
| **14** | 3.8 | 4.0 | **23** | 85 | 30 |
| **15** | 4.4 | 3.2 | **24** | 77 | 17 |
| **16** | 4.2 | 4.8 | **25** | 72 | 20 |
| **17** | 5.2 | 4.9 | **26** | 37 | 22 |

[a] Electrolysis at a controlled potential at the second reduction peak ($Ep_{II}$).

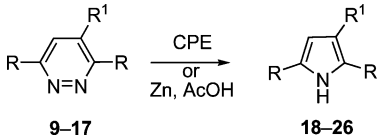


**9–17** **18–26**

Scheme 4.

The electricity consumption of preparative electrochemical reduction, measured by coulometry, corresponded approximately to four electrons per mole of pyridazine, as expected. This was not the case, however, for pyridazines **13** and **17**, which contain an electron-withdrawing substituent ($R^1 = CO_2Et$), where the amount of consumed electrons was significantly higher than 4e$^-$ (5 to 6e$^-$). This latter result suggests that degradation should occur partially in this series.

Thus, yields of isolated 2,5-dipyridin-2- and -4-ylpyrroles **18**–**20** and **23** obtained by electrolysis of pyridazines **9**–**11** and **14**, respectively, were all up to 80%, whereas the transformation of pyridazine **13** ($R^1 = CO_2Et$) into pyrrole **22** was only achieved in a modest 53% yield. The loss of yield observed in the formation of pyrrole **21** from 4-ethoxypyridazine **12** (68%) highlighted the sensitive step of the electrochemical reduction process, occurring at the level of 1,2- and 1,4-dihydro intermediates equilibrium, which seems sensitive to the stronger donor effect of the ethoxy group. The introduction of a methyl substituent on the pyridinyl rings has a surprising influence on the electrochemical synthesis of the corresponding pyrroles and yields 77% of **24**, 72% of **25**, and 37% of **26**, without any trace of 1,4-dihydropyridazine intermediates. By taking into account the previous voltammetry analysis, this observation should be ascribed to the solubility of the latter in the experimental acidic medium.

However, these results also confirm the unfavorable effect of electron-withdrawing groups at C4 of the pyridazine residues on the electrochemical pathway. Nevertheless, all the transformations of pyridazines **9** to **17** are advantageously compared to those obtained by the chemical route, using a Zn/ACOH medium, which afforded the corresponding pyrroles **18**–**26** in only low yields (15 to 30%).

Next, preparative electrolyses were also performed at the potential of the first reduction peak ($Ep_I$) of the pyridazines. These experiments were carried out to investigate whether pyridazines could evolve through the sole dismutation process to the corresponding pyrroles (Scheme 3, Path b). Results with pyridazines **9** ($R^1$ = H), **10** ($R^1$ = Bu), **12** ($R^1$ = OEt), and **13** ($R^1 = CO_2Et$) are presented in Table 4.

Table 4. Coulometric data and yields of substituted pyrroles by electrochemical synthesis. The potential of the first reduction peak $Ep_1$ was applied.

| Pyridazine | F/mol | Time [h] CPE | Pyrrole (yield, %) | Dihydropyridazine (yield, %) |
|---|---|---|---|---|
| **9** | 4.1 | 7.0 | **18** (72) | – |
| **10** | 4.0 | 7.0 | **19** (78) | – |
| **12** | 3.0 | 6.5 | **21** (70) | **27** (12) |
| **13** | 2.1 | 4.1 | **22** (0) | **28** (75) |

  

In the case of pyridazines **9**, **10**, and **12**, four electrons per mol of pyridazine were logically consumed to yield the corresponding pyrroles in over 70% yield. Under these particular electrochemical conditions, the formation of pyrroles supports our ring-contraction mechanism hypothesis. Indeed, 1,2-dihydropyridazine intermediates formed from unsubstituted or electron-donating substituted pyridazines (Scheme 3, Path b) are unstable in acidic medium and undergo a disproportionation process to yield the concomitant formation of pyrroles and starting pyridazines, which can be involved in a further reduction process. Consequently, the reaction time (7 h) was longer than the electrolysis run at the stage of the second reduction wave (5 h). No formation of 1,4-dihydropyridazine was observed during the transformation of **9** and **10**, whereas 4-ethoxy-1,6-dihydropyridazine **27** was identified as an isolable intermediate, in 12% yield, from **12** (Figure 3). The latter was particularly characterized in the $^1$H NMR spectrum by two 1H singlets at $\delta$ = 6.43 and 4.92 ppm.

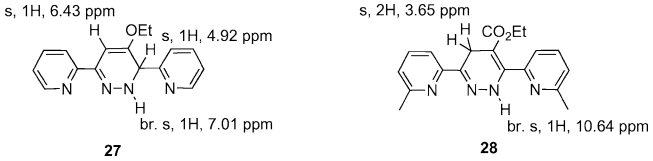


Figure 3. Dihydropyridazine derivatives obtained as a byproduct (**27**) or sole compound (**28**) of the electrochemical reduction run at the potential of the first reduction peak ($Ep_1$) of the corresponding pyridazine **12** and **13**, respectively.

In the presence of electron-withdrawing groups ($R^1$ = $CO_2Et$, **13**), only 2.1 electrons, which correspond to the first potential wave of the pyridazine reduction, were consumed. The formation of pyrrole **22** was then not detected and 1,4-dihydro-5-methoxycarbonylpyridazine derivative **28** (Figure 3) was isolated in 75% yield as the sole product of the reaction. This result shows that the disproportionation process is inhibited in the presence of an electron-withdrawing substituent on the pyridazine ring, and consequently, the 1,2-dihydropyridazine intermediate spontaneously rearranges into a more stable 1,4-dihydropyridazine derivative. The structure of the latter was established by the presence of a 2H singlet for the methylene group at $\delta$ = 3.65 ppm in $^1$H NMR spectroscopy.

Conformational analysis of the 2,5-dipyridin-2-ylpyrrole **18** structures was investigated and it was revealed that, on the one hand, three nonequivalent minima can be found, all of which show coplanar rings ($\phi_{NCCN}$ = 0.0° and 180.0°) as illustrated in Figure 4. On the other hand, transition states TSs present two perpendicular rings ($\phi_{NCCN}$ = 95.0°). The symmetry of this system leads to a symmetric conformational profile (Figure 5) on both sides of the global energetic minimum. This latter (named *syn–syn*) is characterized by the two pyridinyl nitrogen atoms in *syn* position towards the pyrrole nitrogen atom. The two local minima are described by the *anti* position of one (*syn–anti* conformer) or both (*anti–anti* conformer) pyridinyl nitrogen atoms. These rotations result in destabilizations of 14.2 and 35.2 kJ mol$^{-1}$, respectively, by comparison to the absolute minimum. The two similar rotation barriers, found on passing from the *syn–syn* to the *syn–anti* conformer (30.6 kJ mol$^{-1}$), and from the *syn–anti* to the *anti–anti* conformer (33.9 kJ mol$^{-1}$), show that they are surmountable at room temperature. The different conformers are therefore considered to be in equilibrium with each other, and the relative *syn–syn* and *syn–anti* populations are about 99.0 and 1.0%, respectively, whereas the *anti–anti* population can safely be predicted to be present in negligible amounts.

The surprising preferred *syn–syn* structure is explained by the two bifurcated NΛH–N interactions, which are weak but significant intramolecular hydrogen bonds ($d_{NAH}$ = 2.475 Å, 7% shorter than the sum of the van der Waals radii[23]). Conversely, the *syn–anti* rotamer is significantly less stable due to a single hydrogen-bond interaction, despite the fact that it is stronger and slightly more favorable, ($d_{NAH}$ = 2.381 Å, $\theta_{NAH–N}$ = 98.0° against 93.7° in *syn–syn*), and in addition, to a significant repulsion between two close hydrogen atoms ($d_{HAH}$ = 2.178 Å). In contrast, the *anti–anti* rotamer presents two HΛH repulsions and no NΛH–N interaction. The propensity of pyrrole derivatives to form bifurcated hydrogen bonds has previously been underlined.[24] Relative energies between *syn* and *anti* conformers of 2-(pyridin-2-yl)pyrrole and 5-(pyridin-2-yl)-2-(trifluoroacetyl)pyrrole at the B3LYP/6-311G(d,p) level are in good agreement with those found in this work, as well as the geometrical parameters of the intramolecular interactions.

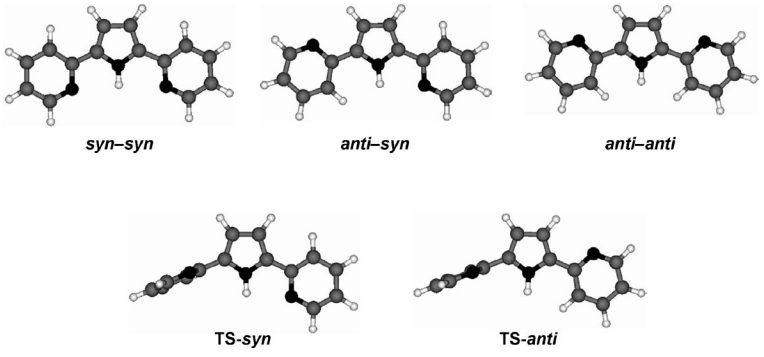


Figure 4. Minima and transition-state conformers of 2,5-dipyridin-2-ylpyrrole **18** found at the MPWB1K/6-31+G(d,p) level.

  

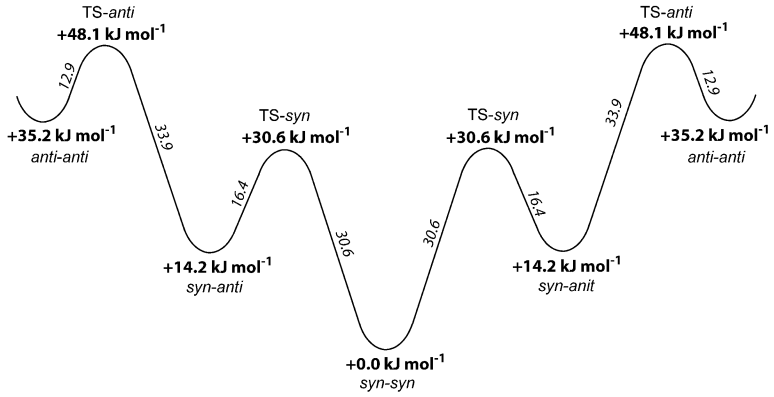


Figure 5. Conformational profile of 2,5-dipyridin-2-ylpyrrole **18** obtained at the LMP2/6-311++G(d,p)//MPWB1K/6-31+G(d,p) level with relative energies and rotation barriers.

Theoretical prediction on the stable conformation of 2,5-dipyridin-2-ylpyrroles was confirmed by X-ray analysis of pyrrole **18**[25] (Figure 6) and compared with dipyridin-4-ylpyrrole analogue **23**[26] (Figure 7), in the solid state.

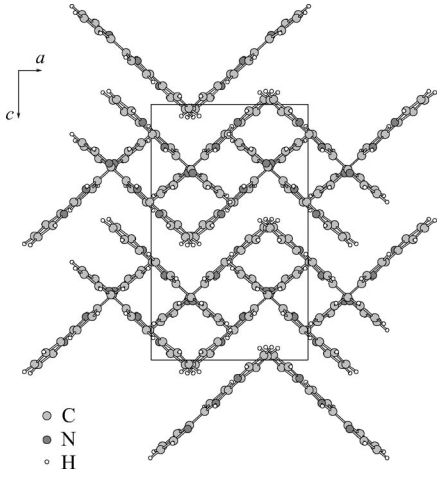


Figure 6. ORTEP diagram of dipyridin-2-ylpyrrole **18**.

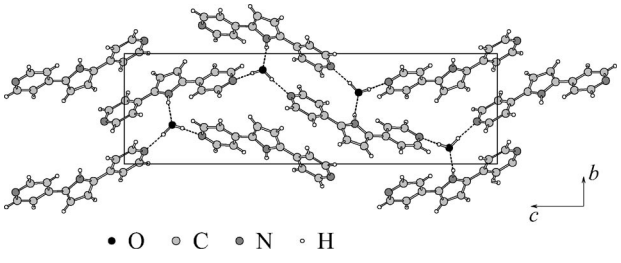


Figure 7. ORTEP diagram of dipyridin-4-ylpyrrole **23**.

In the case of 2,5-dipyridin-4-ylpyrrole **23** (Figure 7), the packing of the $C_{14}H_{11}N_3$ molecules occurs through H-bonded water molecules. Each $C_{14}H_{11}N_3$ molecule is linked to five symmetrically equivalent molecules through three water molecules, which results in a pattern that extends throughout the crystal to give a complex three-dimensional network. In contrast, molecules of 2,5-dipyridin-2-ylpyrrole **18** assemble through van der Waals interactions only (Figure 6). The packing is conveniently obtained by a criss-crossed association, in which the molecules are aligned into two close-to-90° directions to yield double-layer-like substructures.

The experimental conformation observed in the crystalline state is just slightly distorted towards the absolute minimum owing to the packing constraints, with two slightly different orientations of the pyridinyl groups towards the pyrrole ring ($\phi_{NCCN}$ = –0.1 and 12.0°). The superposition of the 17 heavy atoms, which gives an associated RMS deviation of 0.118 Å, illustrates the great similarity of these two structures. The RMS deviation is greatly decreased (0.044 Å) when the superposition is achieved only on the two coplanar rings (Figure 8). In contrast to the theoretical structure, pyridinyl rings show two different bifurcated NΛH–N interactions ($d_{NAH}$ = 2.472 Å and $d_{NAH}$ = 2.574 Å) owing to their nonequivalent orientations. However, the shortest contact is in good agreement with those measured in the optimized *syn–syn* conformer ($d_{NAH}$ = 2.475 Å).

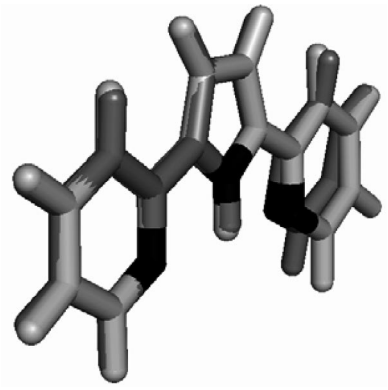

Figure 8. Superposition of the experimental (gray) and the theoretical (pale gray) structures of 2,5-dipyridin-2-ylpyrrole. An RMS deviation value of 0.044 Å was calculated by taking into account the two coplanar rings.

The absorption and the fluorescence properties of the pyridinylpyrrole derivatives were complementarily studied. For all the different pyrroles, the general absorption and

  

fluorescence characteristics were quite similar and no effect of substituents was noticeable.[27] The fluorescence spectra of pyrroles **19**, **24**, **25**, and **26** are exemplified in Figure 9.

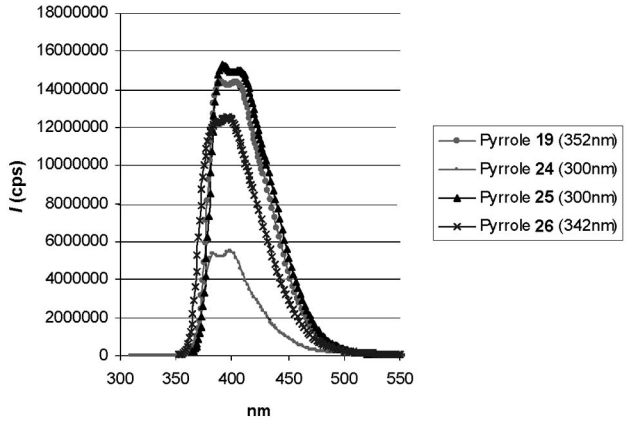


Figure 9. Fluorescence spectra of pyrroles **19**, **24**, **25**, and **26**.

## Conclusions

Results obtained in this study emphasize the potential for substituted pyrroles to be formed by an electroreduction pathway, which was performed from 4-substituted 3,6-dipyridinylpyridazines. The electrochemical ring-contraction process involves four electrons and four protons, in an acidic medium, and is efficient in the presence of pyridinyl groups at the C3 and C6 positions of the pyridazine moiety. Inductive electron-donating groups at the C4 position seem to facilitate the ring-contraction process However, electron-withdrawing groups and mesomeric electron-donating effects affected significantly the formation of pyrroles.

An application of these small pyridinylpyrrolo derivatives in the interaction with the genomic human $tRNAARNt_3^{Lys}$, a natural primer of all immunodeficient viruses, is in course.[29,30] The binding of 2,5-pyridinylpyrrole analogues **18**–**26** on $tRNAARNt_3^{Lys}$ has been evaluated by 600 MHz NMR spectroscopic studies.[28–30] Their selectivity and their ability to be used as inhibitors for reverse transcription of HIV-1 viral RNA will be discussed elsewhere.

## Experimental Section

Solvents were purified and dried by standard methods prior to use.[31] All reactions were carried out under an atmosphere of argon. $^1H$ and $^{13}C$ NMR spectra were recorded with a Bruker AC 300 with TMS as an internal standard for $^1H$ spectra. Chemical shifts ($\delta$) are given in ppm and coupling constants ($J$) in Hz with the following abbreviation for signal multiplicity: s for singlet, br. s for broad singlet, d for doublet, br. d for broad doublet, t for triplet. All reactions were monitored by TLC on commercially available precoated plates (Kieselgel 60 $F_{254}$), and the products were visualized with a Mohr solution (10 g $FeSO_4$ in 100 mL of $H_2O$). Kieselgel 60, 230–400 mesh (Merck), or neutral alumina was used for column chromatography. Mass spectra were measured with a quad. Hewlett Packard 5989A. HRMS were measured with a MS–MS ZABSpec TOF spectrometer from Micromass (Positive Electrospray, solvent: MeOH) and were performed at the "Centre Régional de Mesures Physiques de l'Ouest", Rennes, France. FTIR spectra were obtained in the 500–4000 $cm^{-1}$ range with a Bruker Vector 22 FTIR spectrometer by using NaCl pellets. Fluorescence spectra were recorded with a SPEX Fluoromax fluorimeter.

**General Procedure A. Preparation of 2,6-Dipyridinyl-1,2,4,5-tetrazine:** A solution of cyanopyridine (1 mmol) and hydrazine hydrate (4 mmol), used as solvent, was heated at reflux for 4–5 h (if dissolution of cyanopyridine was difficult few milliliters of EtOH were added to the mixture). After cooling to 0 °C, the expected dihydrotetrazine precipitated and was then filtered and washed with diethyl ether. The yield is quite quantitative.

After dissolution of the dihydrotetrazine in AcOH (20 mL) and $H_2O$ (14 mL), the mixture was cooled to 0 °C. A solution of $NaNO_2$ (10 mmol) in $H_2O$ (2 mL) was then added drop by drop. The reaction mixture immediately turned pink and stirring was pursued for 1 h at 0 °C after the end of the addition. The mixture was then neutralized with an ammonia solution (33% aqueous solution). The precipitate obtained was then filtered, washed with cold water, and dried under high vacuum.

**General Procedure B. [4+2] Cycloaddition Access to Dipyridinylpyridazine:** A solution of tetrazine (1 mmol) and dienophile (2 mmol) in the appropriate solvent (toluene, DMF, or dioxane) was heated for several days (the disappearance of the intense purple color of the tetrazine indicates the progress of the reaction). After evaporation of the solvent under reduced pressure, the crude product was purified by column chromatography on $Al_2O_3$ or by precipitation.

**General Procedure C. Chemical Ring Contraction:** To a solution of pyridazine (1 mmol.) in glacial acetic acid (11 mL) heated at reflux was added activated zinc dust (20 mmol.). The reaction was monitored by TLC. After completion, the mixture was cooled, filtered trough a pad of Celite, and concentrated under reduced pressure. The crude residue was purified by flash chromatography on silica gel.

**General Procedure D. Electrochemical Ring Contraction**

**Cyclic Voltammetry**: Experiments were performed by using a potentiostat–galvanostat EGG PARC Model 273 controlled by the Echem software. A conventional three-electrode system was used with a glassy carbon working electrode, a saturated calomel reference electrode (SCE), and a platinum wire counter electrode.

**Preparative Electrolyses:** Experiments were carried out at a mercury pool electrode (diameter 4.7 cm) at a constant cathodic potential in the two compartments cell separated by a glass frit. The cathodic compartment contained acetic buffer (0.1 mol $L^{-1}$, pH = 4.6, 50 mL), ethanol (50 mL), and the pyridazine substrate ($7 \times 10^{-4}$ mol). Prior to and during electrolysis, the catholyte was deaerated with argon and stirred magnetically. The constant potential (value corresponding to the second reduction peak of the substrates versus the saturated calomel electrode) was imposed by a potentiostat–galvanostat EGG PARC Model 273. The course of the reaction was followed by cyclic voltammetry in the cathodic compartment, and the electrolysis was stopped when the consumption of the starting substrate was completed. After evaporation of ethanol, the aqueous solution was neutralized with $NaHCO_3$ and extracted with $CH_2Cl_2$. When necessary, the pyrrole derivative was purified by column chromatography on alumina.

**Computational Methods:** Owing to their excellent performance-to-cost ratio, the DFT methods constitute a very appealing approach,

  

and new hybrid functionals were developed that include kinetic energy density. The recent MPWB1K functional set up by Truhlar and coworkers[32] proved to outperform the popular B3LYP functional for energy-barrier prediction for kinetics, among others.[32–35] In the present work, we thus selected the MPWB1K functional in conjunction with the 6-31+G(d,p) basis set to establish the conformational profile of 2,5-dipyridin-2-ylpyrrole **18**. The harmonic frequencies were computed to characterize the stationary points (minima vs. TSs) and to estimate the zero-point vibrational energy (ZPVE) corrections and thermodynamic parameters. The population of the various conformers was evaluated from the computed Gibbs energies through a Boltzmann distribution according to the relation:

$$p_i = \frac{e^{-\Delta G_i^o / RT}}{\sum_{i=1}^{n} e^{-\Delta G_i^o / RT}}$$

The studied compound is likely to show stable conformations including intramolecular interactions, and the estimation of the intramolecular basis set superposition error (BSSE) is well known to be a difficult task. It is therefore almost always ignored in the calculations.[36] Consequently, single-point calculations were carried out at the LMP2/6-311++G(d,p)//MPWB1K/6-31+G(d,p) level of theory, as the local MP2 (LMP2) method greatly reduces the BSSE contribution.[37]

All gas phase calculations were performed by using the Gaussian 03[38] and Jaguar[39] packages.

**3,6-Dipyridin-2-yl-1,2,4,5-tetrazine (6):** Compound **6** was synthesized following General Procedure A[40] in 92% yield (3.16 g) from 2-cyanopyridin-2-yl (3.0 g). Purple powder. M.p. 227 °C (ref.[19,20] 229–230 °C).

**3,6-Dipyridin-4-yl-1,2,4,5-tetrazine (7):** Compound **7** was synthesized following General Procedure A in 69% yield (3.3 g) from 2-cyanopyridin-4-yl (4.2 g). Purple powder. M.p. 254 °C (decomp.) [ref.[41] 258 °C (decomp.)]. $^1$H NMR (300 MHz, $CDCl_3$): $\delta$ = 8.96 (dd, $J$ = 1.7, 4.7 Hz, 4 H), 8.45 (d, $J$ = 1.7, 4.6 Hz, 4 H) ppm. $^{13}$C NMR (75 MHz, $CDCl_3$): $\delta$ = 163.7, 151.4, 138.7, 121.6 ppm. NMR was in accordance with the literature data.[42]

**3,6-Bis(6-methylpyridin-2-yl)-1,2,4,5-tetrazine (8):** Compound **8** was synthesized according to General Procedure A in 65% yield (3.4 g) from 2-cyano-6-methylpyridin-2-yl (4.8 g). Purple powder. M.p. 229 °C. $^1$H NMR (300 MHz, $CDCl_3$): $\delta$ = 8.55–8.52 (d, $J$ = 7.7 Hz, 2 H, $H_{pyridine}$), 7,91–7.86 (t, $J$ = 7.8 Hz, 2 H, $H_{pyridine}$), 7,45–7.43 (d, $J$ = 7.8 Hz, 2 H, $H_{pyridine}$), 2.79 (s, 6 H, $CH_3$) ppm. $^{13}$C NMR (75 MHz, $CDCl_3$): $\delta$ = 163.9, 160.2, 149.6, 137.5, 126.4, 121.8, 24.8 ppm. MS: *m*/*z* (%) = 265 (100) $[M]^+$. HRMS (ESI+): calcd. for $C_{14}H_{13}N_6$ $[M + H]^+$ 265.1202; found 265.1207

**3,6-Dipyridin-2-ylpyridazine (9):** Compound **9** was synthesized in 92% yield (215 mg) according to the literature and by following General Procedure B from tetrazine **6** (236 mg) and ethyl vinyl ether (145 mg) in dioxane (reflux, 90 min). Pyridazine **9** was isolated by filtration after cooling the reaction mixture. Yellowish powder. M.p. 178–179 °C (ref.[20,43] 178–180 °C).

**4-Butyl-3,6-dipyridin-2-ylpyridazine (10):** Compound **10** was prepared in 91% yield (559 mg) according to the literature and by following General Procedure B from tetrazine **6** (500 mg) and hexyne (350 mg) in DMF (60 °C, 2 d). Yellowish powder. M.p. 71–72 °C (ref.[20] 70–71 °C).

**4-(1-Hydroxyethyl)-3,6-dipyridin-2-ylpyridazine (11):** Compound **11** was prepared in 71% yield (197 mg) according to the literature from tetrazine **6** (236 mg) and 3-butyn-1-ol (286 mg) in toluene. Yellow powder. M.p. 64 °C (ref.[20] 65–66 °C).

**4-Ethoxy-3,6-dipyridin-2-ylpyridazine (12):** Compound **12** was synthesized following General Procedure B from tetrazine **6** (430 mg) and ethyl ethynyl ether (256 mg) in toluene (5 mL; 60 °C, 5 d). After purification (DCM/petroleum ether, 8:2), pyridazine **12** was isolated in 40% yield (203 mg). Pale-orange crystals. M.p. 141 °C. $^1$H NMR (300 MHz, $CDCl_3$): $\delta$ = 8.77–8.68 (m, 3 H, $H_{pyridine}$), 8.13 (s, 1 H, $H_{pyridazine}$), 7.95–7.81 (m, 3 H, $H_{pyridine}$), 7.40–7.34 (m, 2 H, $H_{pyridine}$), 4.25 (q, $J$ = 7.02 Hz, 2 H, $OCH_2$), 1.47 (t, $J$ = 6.99 Hz, 3 H, $CH_3$) ppm. $^{13}$C NMR (75 MHz, $CDCl_3$): $\delta$ = 159.1, 157.1, 153.9, 153.5, 152.0, 149.3, 149.3, 137.3, 136.5, 125.1, 124.9, 123.7, 122.2, 106.2, 64.7, 14.3 ppm. MS: *m*/*z* (%) = 278 (88) $[M]^+$, 263 (62) $[M - CH_3]^+$, 234 (22) $[M - OEt]^+$, 205 (100) $[M - OEt + N_2]^+$, 78 (54) $[C_5H_4N]^+$. HRMS (ESI+): calcd. for $C_{16}H_{15}N_4O$ $[M + H]^+$ 279.1240; found 279.1245.

**4-Ethoxycarbonyl-3,6-dipyridin-2-ylpyridazine (13):** Compound **13** was synthesized following General Procedure B from tetrazine **6** (400 mg) and ethyl propiolate (345 μL) in toluene (20 mL; 110 °C, 4 d). Pyridazine **13** was isolated, after purification by flash chromatography (ethyl acetate/petroleum ether, 3:7), in 82% yield (425 mg). Yellowish powder. M.p. 101 °C (ref.[21] 100 °C).

**3,6-Dipyridin-4-ylpyridazine (14):** Compound **14** was prepared according to General Procedure B from tetrazine **7** (236 mg) and ethyl vinyl ether (145 mg) in dioxane (reflux, 4 h). Pyridazine **14** was isolated in 93% yield (218 mg) by filtration after cooling the reaction mixture. Pink powder. M.p. 230 °C. $^1$H NMR (300 MHz, $CDCl_3$): $\delta$ = 8.07 (s, 2 H, $H_{pyridazine}$), 8.08–8.04 (m, 4 H, $H_{pyridine}$), 8.86–8.83 (m, 4 H, $H_{pyridine}$) ppm. $^{13}$C NMR (75 MHz, $CDCl_3$): $\delta$ = 156.7, 150.8; 142.8, 124.6, 120.9 ppm. HRMS (ESI+): calcd. for $C_{14}H_{11}N_4$ $[M + H]^+$ 235.0984; found 235.0986.

**3,6-Bis(6-methylpyridin-2-yl)pyridazine (15):** Compound **15** was synthesized by following General Procedure B from tetrazine **8** (3.17 g) and ethyl vinyl ether (1.75 g) in 1,4-dioxane (120 mL; reflux, 90 min). Pyridazine **15** was isolated in 98% yield (3.08 g) by filtration after cooling the reaction mixture. Yellowish powder. M.p. 148 °C. $^1$H NMR (300 MHz, $CDCl_3$): $\delta$ = 8.69 (s, 2 H, $H_{pyridazine}$), 8.57–8.54 (d, $J$ = 8.0 Hz, 2 H, $H_{pyridine}$), 7.81–7.76 (t, $J$ = 7.8 Hz, 2 H, $H_{pyridine}$), 7.28–7.25 (d, $J$ = 7.6 Hz, 2 H, $H_{pyridine}$), 2.67 (s, 6 H, $CH_3$) ppm. $^{13}$C NMR (75 MHz, $CDCl_3$): $\delta$ = 158.3, 137.3, 125.0, 124.2, 118.7, 24.6 ppm. MS: *m*/*z* (%) = 262 (39) $[M]^+$, 233 (48) $[M - N_2 + H]^+$, 142 (62) $[M - N_2 + C_6H_6N]^+$, 92 (54) $[C_6H_6N]^+$. HRMS (EI): calcd. for $C_{16}H_{14}N_4$ 262.1219; found 262.1211.

**4-Butyl-3,6-bis(6-methylpyridin-2-yl)pyridazine (16):** Compound **16** was synthesized by following General Procedure B from tetrazine **8** (444 mg) and hex-1-yne (790 μL) in DMF (30 mL; 80 °C, 48 h). Pyridazine **16** was isolated in 84% yield (449 mg) after purification by flash chromatography (petroleum ether/ethyl acetate, 8:2). Yellowish oil. $^1$H NMR (300 MHz, [D$_6$]DMSO): $\delta$ = 8.42–8.39 (m, 2 H, $H_{pyridine}$, $H_{pyridazine}$), 7.94–7.88 (m, 2 H, $H_{pyridine}$), 7.80–7.74 (d, $J$ = 7.8 Hz, 1 H, $H_{pyridine}$), 7.44–7.39 (t, $J$ = 7.6 Hz, 2 H, $H_{pyridine}$), 3.02–2.95 (t, $J$ = 6.8 Hz, 2 H, $CH_{2butyl}$), 2.61 (s, 3 H, $CH_{3pyridine}$), 2.56 (s, 3 H, $CH_{3pyridine}$), 1.58–1.47 (m, 2 H, $CH_{2butyl}$), 1.35–1.21 (m, 2 H, $CH_{2butyl}$), 0.85–0.77 (t, $J$ = 7.0 Hz, 3 H, $CH_{3butyl}$) ppm. $^{13}$C NMR (75 MHz, DMSO): $\delta$ = 158.9, 158.1, 156.9, 155.1, 152.1, 142.0, 137.8, 137.4, 125.0, 124.5, 123.1, 121.4, 118.2, 31.8, 31.4, 24.2, 24.0, 22.0, 13.5 ppm. MS: *m*/*z* (%) = 318 (54) $[M]^+$, 289 (100) $[M - N_2 + H]^+$, 92 (12) $[C_6H_6N]^+$. HRMS (ESI+): calcd. for $C_{20}H_{23}N_4$ 319.1923; found 319.1923.

**4-Ethoxycarbonyl-3,6-bis(6-methylpyridin-2-yl)pyridazine (17):** Compound **17** was synthesized following General Procedure B

  

from tetrazine **8** (500 mg) and ethyl propiolate (640 μL) in toluene (20 mL; 110 °C, 48 h). Pyridazine **17** was isolated in 97% yield (614 mg) after purification by flash chromatography (petroleum ether/ethyl acetate, 7:3). Pink powder. M.p. 166 °C. $^1$H NMR (300 MHz, $CDCl_3$): $\delta$ = 8.74 (s, 1 H, $H_{pyridazine}$), 8.54 (d, $J$ = 7.8 Hz, 1 H, $H_{pyridine}$), 8.34 (d, $J$ = 7.9 Hz, 1 H, $H_{pyridine}$), 7.82–7.76 (m, 2 H, $H_{pyridine}$), 7.29–7.24 (m, 2 H, H pyridine), 4.43–4.36 (q, $J$ = 7.2 Hz, 2 H, $CH_{2ethoxycarbonyl}$), 2.66–2.58 (s, 6 H, $CH_{3pyridine}$), 1.36–1.33 (t, $J$ = 7.2 Hz, 3 H, $CH_{3ethoxycarbonyl}$) ppm. $^{13}$C NMR (75 MHz, $CDCl_3$): $\delta$ = 166.9, 157.8, 157.5, 156.7, 151.9, 151.2, 136.6, 131.6, 123.9, 123.3, 122.8, 119.3, 118.0, 61.2, 23.8, 23.5, 13.3 ppm. MS: $m/z$ (%) = 334 (7) $[M]^+$, 305 (8) $[M - N_2 + H]^+$, 233 (39) $[M - N_2 + COOEt]^+$, 142 (27) $[M - N_2 + CO_2Et + C_6H_6N + H]^+$, 92 (51) $[C_6H_6N]^+$. IR: $\tilde{\nu}$ = 1727 (C=O) cm$^{-1}$. HRMS (EI): calcd. for $C_{19}H_{18}N_4O_2$ 334.1430; found 334.1421.

**2,5-Dipyridin-2-ylpyrrole (18):** Compound **18** was obtained in 82% yield (167 mg) by electrochemical reduction ($E$ = –1.05 V/ECS, 4.6 h) of pyridazine **9** (215 mg). Yellow crystals. M.p. 91 °C. $^1$H NMR (300 MHz, $CDCl_3$): $\delta$ = 10.52 (br. s, 1 H, NH), 8.53–8.49 (m, 2 H, $H_{pyridine}$), 7.65–7.52 (m, 4 H, $H_{pyridine}$), 7.07–7.00 (m, 2 H, $H_{pyridine}$), 6.75 (d, $J$ = 2.1 Hz, 2 H, $2H_{pyrrole}$) ppm. $^{13}$C NMR (75 MHz, $CDCl_3$): $\delta$ = 150.1, 133.1, 149.1, 136.2, 120.7, 118.3, 108.8 ppm. MS: $m/z$ (%) = 221 (22) $[M]^+$, 220 (100) $[M - 1]^+$. HRMS (ESI+): calcd. for $C_{14}H_{12}N_3$ $[M + H]^+$ 222.1031; found 222.1033.

When the reduction of pyridazine **9** was performed at the potential of the first peak reduction ($E$ = –0.85 V/ECS, 7 h), the corresponding pyrrole **18** was obtained in 72% yield.

**3-Butyl-2,5-dipyridin-2-ylpyrrole (19):** Compound **19** was obtained in 87% yield (173 mg) by electrochemical reduction ($E$ = –1.08 V/ECS, 6 h) of pyridazine **10** (207 mg). Yellow powder. $^1$H NMR (300 MHz, $CDCl_3$): $\delta$ = 10.48 (br. s, 1 H, NH), 8.52 (br. d, $J$ = 4.8 Hz, 1 H, $H_{pyridine}$), 8.56 (br. d, $J$ = 4.8 Hz, 1 H, $H_{pyridine}$), 7.69–7.51 (m, 4 H, $H_{pyridine}$), 7.07–7.01 (m, 2 H, $H_{pyridine}$), 6.64 (d, $J$ = 2.8 Hz, 1 H, $H_{pyrrole}$), 2.82 (t, $J$ = 7.9 Hz, 2 H, $CH_2$), 1.71 (m, 2 H, $CH_2$), 1.52 (m, 2 H, $CH_2$), 0.98 (t, $J$ = 7.3 Hz, 3 H, $CH_3$) ppm. $^{13}$C NMR (75 MHz, $CDCl_3$): $\delta$ = 150.8, 150.2, 149.4, 149.2, 136.3, 136.3, 131.3, 128.7, 126.12, 120.7, 120.3, 119.3, 118.4, 110.2, 32.5, 27.7, 22.8, 14.8 ppm. MS: $m/z$ (%) = 277 (73) $[M]^+$, 248 (100) $[M - C_2H_5]^+$, 234 (64) $[M - CH_2]^+$, 155 (8) $[M - C_5H_4N]^+$, 78 (21) $[C_5H_4N]^+$. HRMS (ESI+): calcd. for $C_{18}H_{20}N_3$ $[M + H]^+$ 278.1657; found 278.1654.

When the reduction of pyridazine **10** was performed at the potential of the first peak reduction ($E$ = –0.85 V/ECS, 7 h), the corresponding pyrrole **19** was obtained in 78% yield.

**3-(1-Hydroxyethyl)-2,5-dipyridin-2-ylpyrrole (20):** Compound **20** was obtained in 92% yield (158 mg) by electrochemical reduction ($E$ = –1.10 V/ECS, 5.3 h) of pyridazine **11** (202 mg). Yellow powder. $^1$H NMR (300 MHz, $CDCl_3$): $\delta$ = 10.33 (br. s, 1 H, NH), 8.48 (br. d, $J$ = 4.8 Hz, 1 H, $H_{pyridine}$), 8.45 (br. d, $J$ = 4.8 Hz, 1 H, $H_{pyridine}$), 7.67–7.61 (m, 2 H, $H_{pyridine}$), 7.59–7.50 (m, 2 H, $H_{pyridine}$), 7.10–7.01 (m, 2 H, $H_{pyridine}$), 6.64 (br. s, 1 H, $H_{pyrrole}$), 3.99 (t, $J$ = 5.9 Hz, 2 H, $CH_2$), 3.06 (t, $J$ = 5.9 Hz, 2 H, $CH_2$) ppm. $^{13}$C NMR (75 MHz, $CDCl_3$): $\delta$ = 150.5, 149.9, 149.0, 148.8, 137.1, 136.6, 132.2, 130.1, 123.3, 120.9, 119.8, 118.7, 110.9, 64.0, 30.4 ppm. HRMS (ESI+): calcd. for $C_{16}H_{16}N_3O$ $[M + H]^+$ 266.1293; found 266.1291.

**3-Ethoxy-2,5-dipyridin-2-ylpyrrole (21):** Compound **21** was obtained in 68% yield (126 mg) by electrochemical reduction ($E$ = –1.18 V/ECS, 5.2 h) of pyridazine **12** (194 mg). Yellow powder. $^1$H NMR (300 MHz, $CDCl_3$): $\delta$ = 10.23 (br. s, 1 H, NH), 8.50 (br. d, $J$ = 4.3 Hz, 1 H, $H_{pyridine}$), 8.47 (br. d, $J$ = 4.3 Hz, 1 H, $H_{pyridine}$), 7.95 (d, $J$ = 8.1 Hz, 1 H, $H_{pyridine}$), 7.63–7.57 (m, 2 H, $H_{pyridine}$), 7.47 (d, $J$ = 8.1 Hz, 1 H, $H_{pyridine}$), 7.05–6.95 (m, 2 H, $H_{pyridine}$), 6.45 (br. s, 1 H, $H_{pyrrole}$), 4.15 (q, $J$ = 6.9 Hz, 2 H, $OCH_2$), 1.48 (t, $J$ = 6.9 Hz, 3 H, $CH_3$) ppm. $^{13}$C NMR (75 MHz, $CDCl_3$): $\delta$ = 149.7, 149.1, 148.6, 148.0, 136.2, 136.2, 120.8, 119.5, 119.4, 118.0, 108.9, 95.6, 66.5, 15.2 ppm. HRMS (ESI+): calcd. for $C_{16}H_{16}N_3O$ $[M + H]^+$ 266.1293; found 266.1293.

When the reduction of pyridazine **12** was performed at the potential of the first peak reduction ($E$ = –0.95 V/ECS, 6.5 h), the corresponding pyrrole **21** was obtained in 70% yield.

**3-Ethoxycarbonyl-2,5-dipyridin-2-ylpyrrole (22):** Compound **22** was obtained in 53% yield (102 mg) by electrochemical reduction ($E$ = –1.00 V/ECS, 6.2 h) of pyridazine **13** (201 mg). Yellow powder. $^1$H NMR (300 MHz, $CDCl_3$): $\delta$ = 10.13 (br. s, 1 H, NH), 8.70 (d, $J$ = 8.1 Hz, 1 H, $H_{pyridine}$), 8.53 (br. d, $J$ = 4.8 Hz, 1 H, $H_{pyridine}$), 8.46 (br. d, $J$ = 4.8 Hz, 1 H, $H_{pyridine}$), 7.69–7.63 (m, 2 H, $H_{pyridine}$), 7.57–7.55 (m, 1 H, $H_{pyridine}$), 7.18 (d, $J$ = 2.2 Hz, 1 H, $H_{pyrrole}$), 7.16–7.03 (m, 2 H, $H_{pyridine}$), 4.29 (q, $J$ = 7.1 Hz, 2 H, $OCH_2$), 1.31 (t, $J$ = 7.1 Hz, 3 H, $CH_3$) ppm. $^{13}$C NMR (75 MHz, $CDCl_3$): $\delta$ = 165.1, 149.4, 148.8, 149.3, 148.9, 136.7, 136.6, 135.6, 131.2, 123.5, 122.6, 121.6, 118.7, 115.0, 111.9, 60.3, 14.5 ppm. HRMS (ESI+): calcd. for $C_{17}H_{16}N_3O_3$ $[M + H]^+$ 294.1243; found 294.1246.

**2,5-Dipyridin-4-ylpyrrole (23):** Compound **23** was obtained in 85% yield (169 mg) by electrochemical reduction ($E$ = –1.00 V/ECS, 4 h) of pyridazine **14** (210 mg). Yellowish crystals. M.p. 261 °C. $^1$H NMR (300 MHz, [D$_6$]DMSO): $\delta$ = 11.81 (br. s, 1 H, NH), 8.57–8.54 (m, 1 H, $H_{pyridine}$), 7.79–7.77 (m, 4 H, $H_{pyridine}$), 6.97 (d, $J$ = 2.1 Hz, 2 H, $2H_{pyrrole}$) ppm. $^{13}$C NMR (75 MHz, [D$_6$]DMSO): $\delta$ = 149.3, 145.5, 136.7, 133.1, 120.7, 118.9, 99.3 ppm. HRMS (ESI+): calcd. for $C_{14}H_{12}N_3$ $[M + H]^+$ 222.1031; found 222.1030.

**3,6-Bis(6-methylpyridin-2-yl)pyrrole (24):** Compound **24** was obtained in 77% yield (135 mg) by electrochemical reduction ($E$ = –1.05 V/ECS, 3.2 h) of pyridazine **15** (184 mg). Yellow powder. M.p. 96 °C. $^1$H NMR (300 MHz, $CDCl_3$): $\delta$ = 10.9 (br. s, 1 H, $NH_{pyrrole}$), 7.54–7.43 (m, 4 H, $H_{pyridine}$), 6.90–6.87 (d, $J$ = 7.4 Hz, 2 H, $H_{pyridine}$), 6.74 (s, 2 H, $H_{pyrrole}$), 2.56 (s, 6 H, $H_3$) ppm. $^{13}$C NMR (75 MHz, $CDCl_3$): $\delta$ = 156.0, 148.6, 137.7, 120.6, 116.3, 110.7, 23.7 ppm. MS: $m/z$ (%) = 249 (100) $[M]^+$, 92 (18) $[C_6H_6N]^+$. IR: $\tilde{\nu}$ = 3443 (NH) cm$^{-1}$. HRMS (ESI+): calcd. for $C_{16}H_{16}N_3$ 250.1344; found 250.1344.

**4-Butyl-3,6-bis(6-methylpyridin-2-yl)pyrrole (25):** Compound **25** was obtained in 72% yield (147 mg) by electrochemical reduction ($E$ = –1.05 V/ECS, 4.2 h) of pyridazine **16** (204 mg). Yellow powder. M.p. 93 °C. $^1$H NMR (300 MHz, $CDCl_3$): $\delta$ = 11.9 (br. s, 1 H, $NH_{pyrrole}$), 7.89–7.85 (m, 3 H, $H_{pyridine}$), 7.67–7.64 (d, $J$ = 7.9 Hz, 1 H, $H_{pyridine}$), 7.23–7.21 (m, 2 H, $H_{pyridine}$), 7.02 (s, 1 H, $H_{pyrrole}$), 2.89–2.84 (t, $J$ = 7.8 Hz, 2 H, $CH_{2butyl}$), 2.65 (s, 3 H, $CH_{3pyridine}$), 2.62 (s, 3 H, $CH_{3pyridine}$), 1.71–1.64 (quint., $J$ = 7.8 Hz, 2 H, $CH_{2butyl}$), 1.50–1.45 (sext., $J$ = 7.2 Hz, 2 H, $CH_{2butyl}$), 1.01–0.97 (t, $J$ = 7.1 Hz, 3 H, $CH_{3butyl}$) ppm. $^{13}$C NMR (75 MHz, $CDCl_3$): $\delta$ = 170.1, 156.9, 149.0, 126.5, 121.0, 120.6, 117.4, 116.5, 112.8, 32.1, 26.6, 23.7, 22.8, 22.1, 13.8 ppm. MS: $m/z$ (%) = 305 (45) $[M]^+$, 92 (46) $[C_6H_6N]^+$. IR: $\tilde{\nu}$ = 3432 (NH) cm$^{-1}$. HRMS (ESI+): calcd. for $C_{20}H_{24}N_3$ 306.1970; found 306.1973.

**4-Ethoxycarbonyl-3,6-bis(6-methylpyridin-2-yl)pyrrole (26):** Compound **26** was obtained in 37% yield (84 mg) by electrochemical reduction ($E$ = –1.05 V/ECS, 9 h) of pyridazine **16** (225 mg). Yellow powder. M.p. 92 °C. $^1$H NMR (300 MHz, $CDCl_3$): $\delta$ = 10.9 (br. s, 1 H, $NH_{pyrrole}$), 8.49–8.46 (d, $J$ = 8.1 Hz, 1 H, $H_{pyridine}$), 7.57–7.47 (m, 2 H, $H_{pyridine}$), 7.38–7.35 (d, $J$ = 8.0 Hz, 1 H, $H_{pyridine}$), 7.14

  

(s, 1 H, $H_{pyrrole}$), 7.01–6.99 (d, 1 H, $H_{pyridine}$), 6.90–6.93 (d, $J$ = 7.5 Hz, 1 H, $H_{pyridine}$), 4.29–4.24 (q, $J$ = 7.1 Hz, 2 H, $CH_{2ethoxycarbonyl}$), 2.55 (s, 3 H, $CH_{3pyridine}$), 2.52 (s, 3 H, $CH_{3pyridine}$), 1.36–1.30 (t, $J$ = 7.1 Hz, 3 H, $CH_{3ethoxycarbonyl}$) ppm. $^{13}$C NMR (75 MHz, $CDCl_3$): $\delta$ = 165.0, 158.0, 157.5, 148.7, 136.8, 136.7, 131.2, 122.1, 120.9, 120.6, 115.6, 114.6, 111.5, 60.1, 24.5, 14.4 ppm. MS: *m*/*z* (%) = 321 (62) $[M]^+$, 275 (100) $[M – EtOH]^+$, 249 (24) $[M – COOEt + H]^+$, 92 (46) $[C_6H_6N]^+$. IR: $\tilde{\nu}$ = 3426 (NH), 1698 (C=O). HRMS (ESI+): calcd. for $C_{19}H_{20}N_3O_2$ 322.1556; found 322.1555.

When the reduction of pyridazine **16** was performed at the potential of the first peak reduction ($E$ = –0.70 V/ECS, 4 h), the corresponding pyrrole **26** was not obtained.

**4-Ethoxy-1,6-dihydro-3,6-dipyridin-2-ylpyridazine (27):** Compound **27** was obtained as a side product in only 12% yield (19 mg) by electrochemical reduction of pyridazine **12** (176 mg) at the first reduction peak potential ($E$ = –0.95 V/ECS, 6.5 h). Orange oil. $^1$H NMR (300 MHz, $CDCl_3$): $\delta$ = 8.59–8.51 (m, 2 H, $H_{pyridine}$), 7.96–7.90 (m, 1 H, $H_{pyridine}$), 7.62–7.55 (m, 2 H, $H_{pyridine}$), 7.30–7.27 (d, $J$ = 7.9 Hz, 1 H, $H_{pyridine}$),7.16–7.13 (m, 2 H, $H_{pyridine}$), 7.01 (br. s, 1 H, NH), 6.43 (s, 1 H, $H_{pyridazine}$), 4.92 (s, 1 H, $H_{dihydropyridazine}$), 4.22–4.14 (q, $J$ = 7.1 Hz, 2 H, $CH_2$), 1.40–1.36 (t, $J$ = 6.9 Hz, 3 H, $CH_3$) ppm.

**4-Ethoxycarbonyl-1,4-dihydro-3,6-dipyridin-2-ylpyridazine (28):** Compound **28** was obtained in 75% yield (161 mg) by electrochemical reduction of pyridazine **13** (214 mg) at the first reduction peak potential ($E$ = –0.70 V/ECS, 4.1 h). Yellow oil. $^1$H NMR (300 MHz, $CDCl_3$): $\delta$ = 10.64 (s, 1 H, NH), 8.67–8.74 (m, 2 H, $H_{pyridine}$), 8.08–8.11 (d, $J$ = 8.0 Hz, 1 H, $H_{pyridine}$), 7.88–7.94 (m, 2 H, $H_{pyridine}$), 7.46–7.56 (m, 3 H, $H_{pyridine}$), 3.84–3.91 (q, $J$ = 7.0 Hz, 2 H, $CH_{2ethoxycarbonyl}$), 3.65 (s, 2 H, $CH_{2dihydropyridazine}$), 0.86–0.91 (t, $J$ = 7.1 Hz, 3 H, $CH_{3ethoxycarbonyl}$) ppm. IR: $\tilde{\nu}$ = 3414 (NH), 1683 (C=O) cm$^{-1}$.

CCDC-648305 (for **23**) and -648306 (for **18**) contain the supplementary crystallographic data for this paper. These data can be obtained free of charge from The Cambridge Crystallographic Data Centre via www.ccdc.cam.ac.uk/data_request/cif.

## Acknowledgments

The authors gratefully acknowledge the CCIPL (Centre de Calcul Intensif des Pays de la Loire), the CINES (Centre Informatique National de l'Enseignement Supérieur), and the IDRIS (Institut Des Ressources en Informatique Scientifique) for computer time.

[1] C.-F. Lee, L.-M. Yang, T.-Y. Hwu, A.-S. Feng, J.-C. Tseng, T.-Y. Luh, *J. Am. Chem. Soc.* **2000**, *122*, 4992–4993.
[2] T. A. Skotheim, R. L. Elsenbaumer, J. R. Reynolds (Eds.), *Handbook of Conducting Polymers*, 2nd ed., Marcel Dekker, New York, **1998**.
[3] A. G. MacDiarmid, *Synth. Met.* **1997**, *84*, 27–34.
[4] R. J. Sundberg, *Comprehensive Heterocyclic Chemistry II* (Eds.: A. R. Katritzky, C. W. Rees, E. F. V. Scriven), Pergamon, Oxford, **1996**, vol. 2, p. 149.
[5] D. L. Boger, C. W. Boyce, M. A. Labroli, C. A. Sehon, Q. Jin, *J. Am. Chem. Soc.* **1999**, *121*, 54–62.
[6] A. Al Mourabit, P. Potier, *Eur. J. Org. Chem.* **2001**, 237–243.
[7] U. Joshi, M. Pipelier, S. Naud, D. Dubreuil, *Curr. Org. Chem.* **2005**, *9*, 261–288 and references cited therein.
[8] G. T. Manh, R. Hazard, J.-P. Pradère, A. Tallec, E. Raoult, D. Dubreuil, *Tetrahedron Lett.* **2000**, *41*, 647–650.
[9] G. T. Manh, R. Hazard, A. Tallec, J.-P. Pradère, D. Dubreuil, M. Thiam, L. Toupet, *Electrochim. Acta* **2002**, *47*, 2833–2841.
[10] D. L. Boger, R. S. Colman, J. S. Panek, D. Yohannes, *J. Org. Chem.* **1984**, *49*, 4405–4409.
[11] D. L. Boger, *Strategies and Tactics in Organic Synthesis* (Ed.: T. Lindberg), Academic Press, **1988**, vol. 2.
[12] D. Dubreuil, M. Pipelier, H. Bakkali, J.-P. Pradère, P. Le Pape, T. Delaunay, A. Tabatchnik, CNRS Patent, PCT/FR2007/001288, **2006**.
[13] D. Dubreuil, M. Pipelier, H. Bakkali, C. Thobie, J.-P. Pradère, E. Léonel, J.-Y. Nédélec, S. Sengamy, T. Delaunay, A. Tabatchnik, CNRS Patent, FR 06 06841, **2006**.
[14] F. Wu, C. M. Chamchoumis, R. P. Thummel, *Inorg. Chem.* **2000**, *39*, 585–590.
[15] W. S. Wilson, R. N. Warrener, *Tetrahedron Lett.* **1970**, 4787–4790.
[16] G. Xiao, A. Kumar, K. Li, C. T. Rigl, M. Bajic, T. M. Davis, D. W. Boykin, W. D. Wilson, *Bioorg. Med. Chem.* **2001**, *9*, 1097–1113.
[17] M. O. Abdel-Rahman, M. A. Kira, M. N. Tolba, *Tetrahedron Lett.* **1968**, *35*, 3871–3872.
[18] R. Nyfeler, P. Ackermann, *ACS Symposium Series (Synth. Chem. Agrochem. III)* **1992**, *504*, 395–404.
[19] W. A. Butte, F. H. Case, *J. Org. Chem.* **1961**, *26*, 4690–4692.
[20] R. Hoogenboom, G. Kickelbick, U. S. Schubert, *Eur. J. Org. Chem.* **2003**, 4887–4896.
[21] M. Ghedini, F. Neve, M. Longeri, M. C. Bruno, *Inorg. Chim. Acta* **1988**, *149*, 131–138.
[22] Polarographic experiments were run on a hanging mercury drop electrode and cyclic voltammetric experiments on a glassy carbon electrode.
[23] A. Bondi, *J. Phys. Chem.* **1964**, *68*, 441–451.
[24] A. V. Afonin, I. A. Ushakov, A. B. I. Mikhaleva, B. A. Trofimov, *Magn. Reson. Chem.* **2007**, *45*, 220–230.
[25] $C_{14}H_{11}N_3$: The data set was collected with a Nonius-Bruker Kappa CCD diffractometer by using Mo-$KL_{2,3}$ radiation. $C_{14}H_{11}N_3$ ($M$ = 221.3): orthorhombic, space group *Pbcn*, $D_{calcd.}$ = 1.333 g cm$^{-3}$, $a$ = 10.8412(12) Å, $b$ = 11.538(2) Å, $c$ = 17.6275(11) Å, $V$ = 2204.9(5) Å$^3$, $Z$ = 8, $\lambda$ = 0.71069 Å, $\mu$ = 0.082 mm$^{-1}$, $T$ = 100 K, $R(F^2)$ = 0.0652 for 2474 observed reflections [$I > 2\sigma(I)$] and $R_w(F^2)$ = 0.1391 for all 3152 reflections. CCDC-648306.
[26] $C_{14}H_{11}N_3 \cdot H_2O$: The data set was collected with a Nonius-Bruker Kappa CCD diffractometer by using Mo-$KL_{2,3}$ radiation. $C_{14}H_{13}N_3O$ ($M$ = 239.3): orthorhombic, space group $P2_12_12_1$, $D_{calcd.}$ = 1.287 g cm$^{-3}$, $a$ = 5.6859(5) Å, $b$ = 8.0090(5) Å, $c$ = 27.1194(16) Å, $V$ = 1234.97(15) Å$^3$, $Z$ = 4, $\lambda$ = 0.71069 Å, $\mu$ = 0.084 mm$^{-1}$, $T$ = 120 K, $R(F^2)$ = 0.0471 for 4698 observed reflections [$I > 2\sigma(I)$] and $R_w(F^2)$ = 0.1141 for all 5212 reflections. CCDC-698305.
[27] L. A. MacManus-Spencer, S. J. Schmidtke, D. A. Blank, K. McNeill, *Phys. Chem. Chem. Phys.* **2004**, *6*, 3948–3957.
[28] P. Plateau, M. Gueron, *J. Am. Chem. Soc.* **1982**, *104*, 7310–7311.
[29] C. Tisne, B. P. Roques, F. Dardel, *J. Mol. Biol.* **2001**, *306*, 443–454.
[30] C. Tisne, B. P. Roques, F. Dardel, *Biochimie* **2003**, *85*, 557–561.
[31] D. D. Perrin, W. L. F. Amarego, *Purification of Laboratory Chemicals*, Pergamon, Oxford, **1988**.
[32] Y. Zhao, D. G. Truhlar, *J. Phys. Chem. A* **2004**, *108*, 6908–6918.
[33] Y. Zhao, D. G. Truhlar, *J. Phys. Chem. A* **2005**, *109*, 6624–6627.
[34] Y. Zhao, D. G. Truhlar, *J. Phys. Chem. A* **2005**, *109*, 5656–5667.
[35] Y. Zhao, D. G. Truhlar, *J. Phys. Chem. A* **2005**, *1*, 415–432.
[36] F. Jensen, *Introduction to Computational Chemistry*, Wiley, New York, **1999**.
[37] S. Saebo, W. Tong, P. Pulay, *J. Chem. Phys.* **1993**, *98*, 2170–2175.
[38] M. J. Frisch, G. W. Trucks, H. B. Schlegel, G. E. Scuseria, M. A. Robb, J. R. Cheeseman, J. A. Montgomery, J. T. Vreven, K. N. Kudin, J. C. Burant, J. M. Millam, S. S. Iyengar, J. Tomasi, V. Barone, B. Mennucci, M. Cossi, G. Scalmani, N. Rega, G. A. Petersson, H. Nakatsuji, M. Hada, M. Ehara, K. Toyota,

  

R. Fukuda, J. Hasegawa, M. Ishida, T. Nakajima, Y. Honda, O. Kitao, H. Nakai, M. Klene, X. Li, J. E. Knox, H. P. Hratchian, J. B. Cross, C. Adamo, J. Jaramillo, R. Gomperts, R. E. Stratmann, O. Yazyev, A. J. Austin, R. Cammi, C. Pomelli, J. W. Ochterski, P. Y. Ayala, K. Morokuma, G. A. Voth, P. Salvador, J. J. Dannenberg, V. G. Zakrzewski, S. Dapprich, A. D. Daniels, M. C. Strain, O. Farkas, D. K. Malick, A. D. Rabuck, K. Raghavachari, J. B. Foresman, J. V. Ortiz, Q. Cui, A. G. Baboul, S. Clifford, J. Cioslowski, B. B. Stefanov, G. Liu, A. Liashenko, P. Piskorz, I. Komaromi, R. L. Martin, D. J. Fox, T. Keith, M. A. Al-Laham, C. Y. Peng, A. Nanayakkara, M. Challacombe, P. M. W. Gill, B. Johnson, W. Chen, M. W. Wong, C. Gonzalez, J. A. Pople, *Gaussian 03*, Version RevD.02, Gaussian, Inc., Wallingford, CT, **2004**.

[39] L. L. C.Schrödinger, *Jaguar*, Version 6.0, New York, **2005**.

[40] J. F. Geldard, F. Lions, *J. Org. Chem.* **1965**, *30*, 318–319.

[41] D. D. Libman, R. Slack, *J. Chem. Soc.* **1956**, 2253–2257.

[42] P. H. Dinolfo, M. E. Williams, C. L. Stern, J. T. Hupp, *J. Am. Chem. Soc.* **2004**, *126*, 12989–13001.

[43] V. G. Kumar Das, L. K. Mun, C. Wei, S. J. Blunden, T. C. W. Mak, *J. Organomet. Chem.* **1987**, *322*, 163–175.

Received: November 26, 2007
Published Online: March 13, 2008
(since its publication in Early View, a minor change in one of the co-authors' names has been made.)

  